OXFORD

Human Molecular Genetics, 2017, Vol. 0, No. 0 1–13

doi: 10.1093/hmg/ddx355
Advance Access Publication Date: 14 September 2017
Original Article

ORIGINAL ARTICLE

Neurodevelopmental disease-associated *de novo* mutations and rare sequence variants affect TRIO GDP/GTP exchange factor activity

Sara M. Katrancha[1,2,3], Yi Wu[4], Minsheng Zhu[5], Betty A. Eipper[6,7], Anthony J. Koleske[1,2,3] and Richard E. Mains[6,*]

[1]Interdepartmental Neuroscience Program, [2]Department of Neuroscience and [3]Department of Molecular Biophysics and Biochemistry, Yale University, New Haven, CT, USA, [4]Center for Cell Analysis and Modeling, University of Connecticut Health Center, Farmington, CT, USA, [5]Model Animal Research Center, Nanjing University, Nanjing 210061, China, [6]Department of Neuroscience and [7]Department of Molecular Biology and Biophysics, University of Connecticut Health Center, Farmington, CT, USA

*To whom correspondence should be addressed at: Neuroscience Department, University of Connecticut Health Center, 263 Farmington Avenue, Farmington, CT 06030-3401, USA. Tel: +1 8606798894; Fax: +1 8606791060; Email: mains@uchc.edu

Abstract

Bipolar disorder, schizophrenia, autism and intellectual disability are complex neurodevelopmental disorders, debilitating millions of people. Therapeutic progress is limited by poor understanding of underlying molecular pathways. Using a targeted search, we identified an enrichment of *de novo* mutations in the gene encoding the 330-kDa triple functional domain (TRIO) protein associated with neurodevelopmental disorders. By generating multiple TRIO antibodies, we show that the smaller TRIO9 isoform is the major brain protein product, and its levels decrease after birth. TRIO9 contains two guanine nucleotide exchange factor (GEF) domains with distinct specificities: GEF1 activates both Rac1 and RhoG; GEF2 activates RhoA. To understand the impact of disease-associated *de novo* mutations and other rare sequence variants on TRIO function, we utilized two FRET-based biosensors: a Rac1 biosensor to study mutations in TRIO (T)GEF1, and a RhoA biosensor to study mutations in TGEF2. We discovered that one autism-associated *de novo* mutation in TGEF1 (K1431M), at the TGEF1/Rac1 interface, markedly decreased its overall activity toward Rac1. A schizophrenia-associated rare sequence variant in TGEF1 (F1538Intron) was substantially less active, normalized to protein level and expressed poorly. Overall, mutations in TGEF1 decreased GEF1 activity toward Rac1. One bipolar disorder-associated rare variant (M2145T) in TGEF2 impaired inhibition by the TGEF2 pleckstrin-homology domain, resulting in dramatically increased TGEF2 activity. Overall, genetic damage to both TGEF domains altered TRIO catalytic activity, decreasing TGEF1 activity and increasing TGEF2 activity. Importantly, both GEF changes are expected to decrease neurite outgrowth, perhaps consistent with their association with neurodevelopmental disorders.

Introduction

Bipolar disorder, schizophrenia, autism and intellectual disability are complex neurodevelopmental disorders that debilitate ~2.6% (1), 1.1% (2), 1.5% (3) and 1.0% (4) of individuals in the USA, respectively, and millions more worldwide. Current therapies do not fully ameliorate neurological disease symptoms. In particular, while pharmacologic therapies for schizophrenia and bipolar disorder can improve positive symptoms, they often

Received: June 17, 2017. **Revised:** August 7, 2017. **Accepted:** August 22, 2017

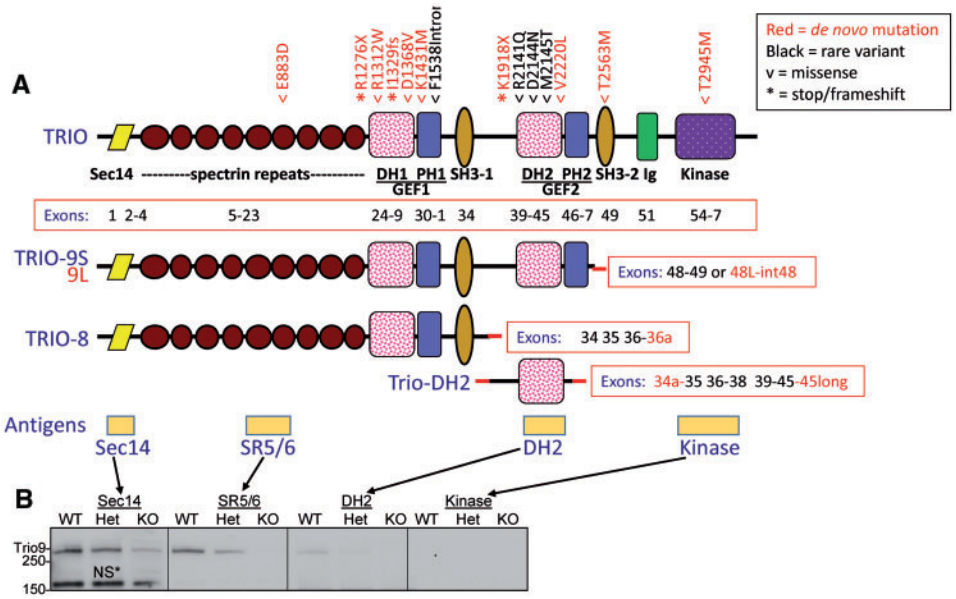

Figure 1. TRIO Isoforms and Disease-Associated Mutations and Variants. **(A)** TRIO and abundant shorter isoforms are diagrammed based on McPherson *et al.* (34) and Tilgner *et al.* (65). The positions of disease-associated *de novo* mutations (in red) and rare sequence variants (in black) are denoted by 'v' (missense) and '*' (stop codon/frameshift) (12,17,19–21, 23–28,55–59). Antigen locations are noted. **(B)** Forebrain tissue was collected from male mice at postnatal day (P) 21; sonicated continuously for 20 s in 50 mM Tris, 1% SDS, 2 mM EDTA, pH 8.0 with protease inhibitors; and boiled for 5 min. Equal protein (30 μg) was loaded on each lane of an SDS polyacrylamide gradient gel. Conditional TRIO knockout mice (62,63) were crossed with *NEX-Cre* mice under the *Neurod6* promoter (64). WT includes tissue from *NEX-Cre*+/− and *Trio*+/+ mice; Het is *NEX-Cre*+/− *Trio*+/*fl*; KO is *NEX-Cre*+/− *Trio fl/fl*. NS* indicates a non-specific band (for this to be a genuine TRIO isoform of ∼165 kDa, it would be detectable with the SR5/6 antibody).

fail to improve negative or cognitive symptoms, including deficits in social interactions, affective experience and clarity of thought (5,6). Similarly, predominant therapies for autism and intellectual disability do not address underlying cognitive abnormalities, but rather include specialized behavioral interventions and pharmacologic treatments for comorbid conditions, such as depression or anxiety (7). There is a critical need for new therapeutic interventions, but progress is limited by a poor understanding of the molecular and cellular pathways underlying neurodevelopmental disorders.

For each of these disorders, genetic and environmental risk factors are believed to disrupt normal cognition and alter neuronal connectivity, as exemplified by alterations in dendrite and dendritic spine structure (8–11). For example, dendritic spines, the main receptive contacts for glutamatergic synapses, are significantly reduced in the prefrontal cortices of individuals with bipolar disorder (8) and schizophrenia (9), and increased across multiple cortices in individuals with autism spectrum disorders (10). Furthermore, a high degree of genetic overlap has been noted among these disorders, especially in genes related to synaptic stability and function (12–17), suggesting disruptions of common molecular mechanisms (18). An abundance of neurologic disease-associated *de novo* mutations and rare sequence variants have been identified in the triple functional domain (*TRIO*) gene (12,17,19–32), including both missense and protein-truncating variants (Fig. 1A).

The mammalian *TRIO* gene encodes a 330-kDa protein; as depicted in Figure 1A, tissue-specific alternative splicing generates multiple isoforms (33–38). Full length TRIO has three catalytic domains: two guanine nucleotide exchange factor (GEF) domains and a predicted serine/threonine kinase domain. TRIO GEF1 activates both Rac1 and RhoG while GEF2 activates RhoA (33,39,40). TRIO also has accessory domains for protein–protein and protein–lipid interactions, including a Sec14 domain, spectrin repeats, two Src-homology 3 domains (SH3), and an immunoglobulin-like (Ig) domain (34,41–44). Of particular interest, studies in diverse model organisms, including *Caenorhabditis elegans*, *Drosophila melanogaster* and mice, as well as human patients, have described important roles for the TRIO family GEF domains in the regulation of dendrite, dendritic spine, and synapse development and function (29,45–47). KALIRIN, a vertebrate paralog of TRIO, is also implicated in human neurological disease and is known from studies in rodents to regulate dendrite and dendritic spine stability (14,48–54). Overall, because of the association of *TRIO* with neurological disease and its known role in dendrite development (29), analyzing the impact of variants on TRIO function will improve our understanding of neurodevelopmental disorders that are characterized by dendrite and dendritic spine abnormalities, such as bipolar disorder (8), schizophrenia (8,9), autism (10) and intellectual disability (11).

This study aims to identify and enumerate *TRIO de novo* mutations associated with neurodevelopmental disorders, characterize TRIO protein expression in the brain, and analyze the impact of *de novo* mutations and rare sequence variants on TRIO protein function. We discovered that *TRIO* contains more protein-coding mutations than expected by random chance, revealed that the TRIO9 isoform is expressed in both human and rodent brain, and showed that TRIO9 levels decrease during development. Furthermore, we prioritized neurodevelopmental disease-associated GEF1 and GEF2 mutations/variants, shown in Figure 1A, based on their potential to impact activity and tested them alongside control variants in GTPase activity assays. While none of the control variants had a major impact on activity, several mutants contained stop codons immediately before the TRIO GEF1 or GEF2 domain and 3 of the remaining 12 mutations/variants showed major changes in GEF activity. Importantly, these three TRIO GEF changes are expected to decrease neurite outgrowth, perhaps consistent with their association with neurodevelopmental disorders.

Results

TRIO contains more *de novo* protein-coding mutations than expected by random chance

De novo mutation and exome sequencing analyses have revealed an abundance of protein-coding mutations and variants associated with neurodevelopmental disorders, including schizophrenia (12,17,19–21,55,56), autism (22–25,57–59), intellectual disability (26,27,29), bipolar disorder (56) and epileptic encephalopathy (28). The *TRIO* gene (ENSG00000038382) is particularly interesting, as exome sequencing analyses on control populations have classified *TRIO* as 'highly constrained', containing significantly fewer rare missense (60) variants and one sixth the number of protein-truncating variants (61) than expected for a transcript of its size. These data suggest a sensitivity or intolerance of *TRIO* to mutational changes, making observed mutations highly likely to contribute to disease. To evaluate neurological case-associated genetic variation, *de novo* mutations are particularly revealing, as these genetic alterations occur for the first time in the affected individual and are not inherited from either unaffected parent. To analyze protein-coding *de novo* mutations in the TRIO protein, a targeted search of *de novo* mutation studies was performed for schizophrenia (12,17,19–21,55), autism (23–25,57–59), intellectual disability (26,27) and epileptic encephalopathy (28). Along with published studies, this targeted search also included *de novo* mutations in *TRIO* from an unpublished exome-sequenced cohort from Taiwan, consisting of 1695 individuals diagnosed with schizophrenia and their unaffected parents (D. Howrigan and B. Neale, personal communication).

From this collection of exomes from neurodevelopmental disorder triads (affected child; unaffected parents), we observed 7 missense, 1 frameshift and 2 nonsense *de novo* mutations across 7208 independent triads (Fig. 1A and Table 1). Based on the mutation model expectation derived in Samocha *et al.* (60), we expected 1.56 missense or protein-truncating mutations in *TRIO* under a null model of no association. Using a Poisson distributed model, the probability of observing 10 *de novo* mutations in the *TRIO* gene is highly unlikely [Table 1, P-value $= 5.60 \times 10^{-06}$ for 10 mutations in 7208 triads; also see Jiang *et al.* (13)], despite not surpassing exome-wide multiple testing correction [set at 1×10^{-06} in Samocha *et al.* (60)]. Across the range of neurodevelopmental disorders investigated, the observed number of *TRIO de novo* mutations, if assumed fully penetrant in all affected probands, is estimated to explain 1 in 721 cases. This enrichment of *de novo* mutations in *TRIO* by itself strongly suggests an association with neurodevelopmental disease. In addition, other studies have shown *TRIO* at or near the significance threshold for an association with neurodevelopmental disorders (13,31,32), making *TRIO* a strong candidate for functional follow-up. Furthermore, many neurologic case-associated rare sequence variants were identified in the *TRIO* gene in Genovese *et al.* (56). We tested a subset of *TRIO* variants from this study that were not observed in controls in the Exome Aggregation Consortium (ExAc) database (http://exac.broadinstitute.org/) and were algorithmically and structurally predicted to be damaging. Of particular interest, the TRIO GEF domains contained the highest density of neurological case-associated *de novo* mutations and several rare sequence variants in the whole *TRIO* gene (Fig. 1A).

Using PolyPhen2, Provean and other prediction algorithms, a large number of these mutations and variants were predicted to damage TRIO function (Table 3). To study the actual impact on protein function, we developed and tested TRIO constructs containing the most potentially damaging mutations and variants, as identified by the specific amino acid change, amino acid location and predicted impact. The truncation mutants (R1276stop; K1918stop) were treated as equivalent to the addition of no exogenous GEF. Some non-case-associated variants (I1329F, I1329S,

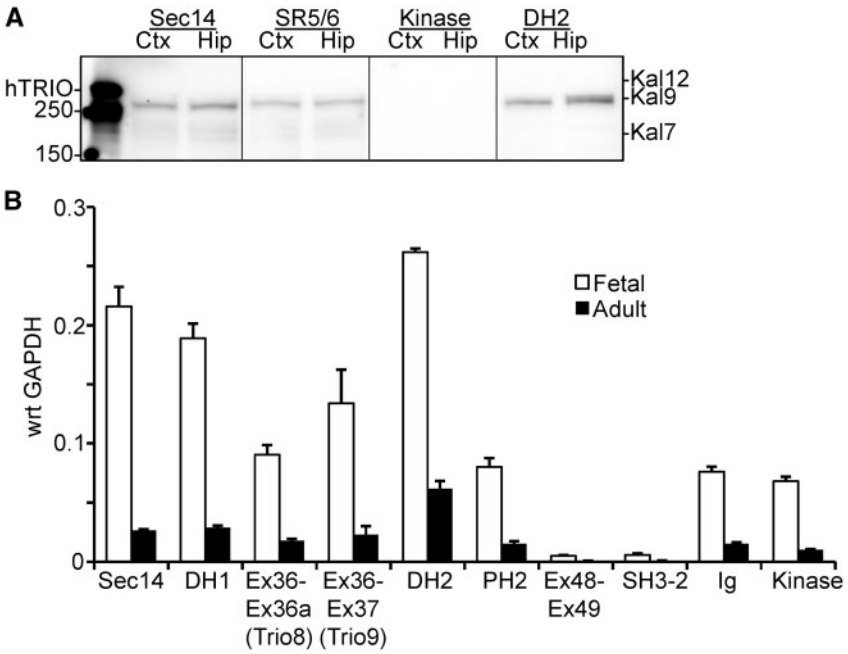

Figure 2. TRIO isoform expression in human brain. **(A)** SDS extracts of adult human cortex and hippocampus (30 μg protein; Takara/Clontech) were analyzed on SDS polyacrylamide gradient gels with recombinant human TRIO included in the molecular weight standard lane. Kalirin antisera were used to detect Kal7, Kal9 and Kal12 in an additional lane of human cortical extract; molecular weights of standards (kDa) are indicated (67). **(B)** qPCR averaged across 8 assays of human fetal and adult brain cDNA; primer locations are indicated (see Fig. 1A and Table 2). In each assay, GAPDH was also assayed for every sample, and data are expressed relative to GAPDH; bars show mean ± SEM.

Table 1. TRIO *de novo* mutation analysis

Neurodevelopmental disorder	Number of triads analyzed per disorder	Observed *de novo* mutation	TRIO protein domain
Schizophrenia	2720	R1276X	Before GEF1
		K1918X	Before GEF2
Autism	3982	R1312W	GEF1
		I1329fs	GEF1
		K1431M	GEF1
		V2220L	GEF2
		E883D	Spectrin repeats
Intellectual disability	151	D1368V	GEF1
		T2563M	SH3(2)
Epileptic encephalopathy	356	T2945M	Kinase

Protein-coding *de novo* mutations in the TRIO protein were analyzed using published studies of schizophrenia (12,17,19–21,55), autism (23–25,57–59), intellectual disability (26,27) and epileptic encephalopathy (28) and one unpublished exome-sequenced schizophrenia cohort from Taiwan, consisting of 1695 triads (D. Howrigan and B. Neale, personal communication). Seven missense, 1 frameshift, and 2 stop-gained *de novo* mutations were observed across 7208 independent triads. This table contains a breakdown of triads per disease, the specific amino acid changes, and the affected TRIO protein domain for the *de novo* mutations. Based on the mutation model expectation derived in Samocha *et al.* (60), we expect 1.56 missense or protein-truncating mutations in *TRIO* under a null model of no association. Using a Poisson distributed model, the *TRIO* gene exhibits an enrichment of *de novo* mutations in neurodevelopmental disorders (P-value=5.60×10^{-06} for 10 mutations in 7208 triads), strongly suggestive of an association with neurological disease, despite not surpassing exome-wide multiple testing correction [set at 1×10^{-06}; Samocha *et al.* (60)]. X, stop/termination codon; GEF, guanine nucleotide exchange factor; SH3, SRC Homology 3; fs, frameshift.

Table 2. qPCR primers

Transcript Name and Description	Oligo Name	Oligo Sequence	Tm(°C)	Length(nt)
GAPDH	hGAPDH-for	TCAGCAATGCCTCCTGCACCACC	61	120
	hGAPDH-rev	TCTTCTGGGTGGCAGTGATGGCATG	61	
TRIO Sec14	tSec14-for	CCTGTATTCCCAGCGAGGAGGTC	61	130
	tSec14-rev	ACATGGATGCAGCAGGGGAAGGAC	61	
TRIO DH1	tDH1-for	ACCAGTTCAGCGAATAACGAAATATCAGCTC	60	128
	tDH1-rev	CGTCATTGGCTCGCTTCGGCACG	62	
TRIO Exon 36–36a	tExon36-for	CCGCCACCCATGGCCATCCA	60	120
	tEx36a-rev	TCAAACGGAAAGGTAAGGAAATTGAGCCAAAAC	62	
TRIO Exon 36–37	tExon36-for	CCGCCACCCATGGCCATCCA	60	120
	tExon37-rev	GAGCTCGGCTGCACTCGGTGTTT	61	
TRIO DH2	tDH2-for	GTTTTGCAAGAACTAGTGGAGACAGAGCGT	61	121
	tDH2-rev	GTCTTTTCCTTTCATGTCATCAGGAACACCATC	61	
TRIO PH2	tPH2-for	GTGCAACGACATGATGAACGTGGGG	60	124
	tPH2-rev	GGCAGAAGTCCTGCATCTTGGTCTG	60	
TRIO Exon 48–49	tExon48-for	AGCCGGCCCTCCCGGATCC	62	125
	tExon49-rev	AGATGTTGCTACTGCTGCTGCTTTCACTC	61	
TRIO SH3-2	tSH3-2-for	ATCTCCACCATGTTGGTGACACACGATTAC	62	121
	tSH3-2-rev	CGGAACACCAGAAACATGTTCTGCTGGT	61	
TRIO Ig	tIg-for	TGAGGTCACGTGTGAGACAGGGG	61	121
	tIg-rev	GTAGTGACCATCGTTGTTCAAGGTGTTGTGT	61	
TRIO Kinase	tKin-for	GAAGATCAGGGCGCACCTGGGG	62	125
	tKin-rev	GGCTTGGCTAAACTCTCATCCACC	61	

Quantitative polymerase chain reaction primers were designed to have calculated melt temperatures of 60–62 °C and a product length of 120–130 bp (67); data are normalized to the GAPDH signal for each sample and averaged across assays (67).

D2113N) were tested as controls for our assays and the mutagenesis process. To complement the PolyPhen2 and Provean predictions, we used Clustal and structure-based analyses to prioritize variants by the structural considerations that could impact function; for example, we tested R2141W and V2220G instead of R2141Q or V2220L. Furthermore, some variants identified in affected individuals were not tested, because they were at sites that tolerate several residues by Clustal analysis across multiple species or were in aqueous loops away from known protein–protein interfaces (L1439M, S1459G, R2086C, K2119E). To evaluate the effects of these mutations and variants, we first needed to identify the major TRIO isoforms expressed in the human brain and the developmental time course over which *TRIO* is expressed.

Characterization of TRIO isoform expression in human and rodent brain

To investigate TRIO protein expression in rodent and human brain tissues, we generated rabbit antibodies for the Sec14, spectrin repeat 5/6 (SR5/6), GEF2 and putative kinase domains of human TRIO (Fig. 1B). Antibodies were validated using cortical

extracts from mice harboring a conditional TRIO knockout (62,63) crossed with *NEX-Cre* mice under the *Neurod6* promoter (64); *Neurod6* expression is limited to excitatory neurons in the cerebral cortex (64). The SR5/6, Sec14 and GEF2 antisera all detected the same overlapping pair of bands (268 and 289 kDa) in rodent cortex, corresponding in size to TRIO9S and TRIO9L, respectively (34) (Fig. 1A). These bands are decreased in intensity in the heterozygote and largely ablated in the homozygote TRIO knockout mouse (Fig. 1B). Consistent with this conclusion, the TRIO kinase antibody, which detects recombinant TRIO (not shown), failed to detect a protein of this mass or any other large product in rodent cortical samples (Fig. 1B); this result corresponds to previous findings with an independent kinase domain antibody (34).

We next used these antisera to identify the TRIO isoforms present in adult human cortex and hippocampus, brain regions with the highest levels of TRIO (Brainspan; Allen Brain Atlas) (Fig. 2A); the samples analyzed were commercially prepared and included a mixture of adult male and female tissue. A major band the size of TRIO9 was detected by the same three antisera but not by kinase domain antibodies, while full-sized recombinant TRIO (analyzed in a parallel lane) was detected by all of the antibodies.

To assess developmental regulation of TRIO expression in humans, cDNAs were prepared from commercial samples: two samples were from adult tissue and two were from fetal samples. Amplicons spanning full-length TRIO were examined (Fig. 1). Normalized to the GAPDH internal standard, each amplicon in the fetal sample was present at significantly higher levels relative to adult, with a consistent 6.6 ± 1 ratio of fetal to adult signal across 20 primer sets spanning the TRIO protein. Ten of these quantitative polymerase chain reaction (qPCR) primer sets, presented in Figure 2B, revealed comparable amounts of Sec14 domain, GEF1 (DH1) domain, TRIO8 COOH-terminus and GEF2 domain transcripts. Consistent with the immunoblot data, the qPCR analysis revealed virtually no signal for the Exon 48–49 and SH3-2 regions, which would connect GEF2 to the kinase domain, as in Tilgner *et al.* (65). Based on both western blot analysis and qPCR, TRIO9 is the major isoform expressed in human cortex and hippocampus.

TRIO isoform levels during development and subcellular localization

To better understand developmental changes in TRIO levels, we prepared extracts from mouse cortex from birth to 6 months of age. Analyzing equal amounts of protein from each age, we found that TRIO9 levels gradually decreased with age (Fig. 3A); as a positive control, recombinant TRIO was always detected on the same gel (+TRIO). Expression of postsynaptic density (PSD) protein 95 (PSD95), a marker for the formation of excitatory synapses was also evaluated; as expected, PSD95 levels increased dramatically between postnatal day 7 and postnatal day 31, the time period of maximum synaptogenesis and synaptic pruning (66). The level of heat shock protein 70 (HSP70) was constant across development.

Since one key to protein function is localization, the subcellular distribution of TRIO proteins was investigated in adult mouse cortex (Fig. 3B). For comparison, the subcellular localization of the protein made from the 7 kb splice variant of the *KALRN* gene (Kal7), which is largely localized to the postsynaptic density (67), was evaluated. Equal amounts of protein from each fraction were analyzed. The TRIO antibodies detected proteins the size of TRIO9 (S and/or L) in each fraction. A substantial amount of TRIO was present in the cytosol and the lysed synaptosomes (LS1), indicating that it was soluble. TRIO9 was also recovered from the P3 fraction, which is enriched in endoplasmic reticulum, and in the P2 or synaptosomal membrane fraction. After gradient purification, the PSD-enriched pellet was fractionated into Triton X-100 (TX-100) soluble proteins and purified PSDs. Although TRIO9 was recovered in synaptosomal membranes, with one variant solubilized by TX-100 and the other remaining in the PSDs, TRIO9 was not enriched in the purified PSDs. Kal7, like GluN2B and PSD95, was substantially enriched in purified PSDs [as in Miller *et al.* (67)].

Overall, our finding that the TRIO9 isoform predominates in human and rodent brain early in development is consistent with published studies establishing that TRIO levels in several brain regions drop after birth, suggesting it plays a major developmental role (35,47,62,68–70). Furthermore, both Rac1 and RhoA, which are activated by the TRIO GEF1 and GEF2 domains, respectively, play central roles in controlling the cytoskeletal rearrangements that power nervous system development (71), highlighting the importance of understanding the impact of mutations and rare variants on the function of these domains for neurodevelopmental disorders.

Disease-associated variants in the TRIO GEF1 domain reduce its activity

To assess the impact of *de novo* mutations and rare sequence variants in the TGEF1 domain on protein stability and catalytic activity, we established a quantitative cell-based biosensor assay for the activation of Rac1. The Rac1 bioassays use a fluorescence resonance energy transfer- (FRET-)based biosensor in which activation of Rac1 enables intra-sensor interactions with its binding partner PAK. The Rac1 activation-induced conformational change promotes FRET between the cyan fluorescent protein (CFP) and yellow fluorescent protein (YFP) within the biosensor, leading to increased emission at 525 nm (72,73). The emission spectra for HEK293 cells transfected with the Rac1 biosensor and selected TGEF1 constructs are shown in Figure 4A. Transfection of increasing amounts of wild-type (WT) TGEF1 yielded a dose-dependent increase in Rac1 biosensor FRET, as observed with similar KALIRIN GEF1 constructs (67,73).

To quantify the difference in the relative activity of the constructs toward Rac1, cells were transfected with a constant amount of biosensor and increasing amounts of the various TGEF1 expression constructs. Western blot analyses were performed from a portion of the extracts of transfected HEK293 cell lysate (Fig. 4C), to relate the Rac1 biosensor activity to relative TGEF1 protein levels. The FRET signal at 525 nm obtained for each well was normalized to relative TGEF1 protein levels, as determined by immunoblotting (Fig. 4D). The dose-dependent response of the R1312W, I1329S, I1329F, D1368V and D1368Y variants were indistinguishable from WT TGEF1 (Fig. 4D); the R1312 and D1368 mutations were case-associated variants (Table 1), while the I1329 mutations were chosen as controls. In contrast, two of the tested disease-associated TGEF1 variants substantially reduced the ability of the protein to activate Rac1: K1431M and F1538Intron (Fig. 4A). The autism-associated K1431M *de novo* mutant was only 8% as active as WT TGEF1 when normalized to protein level ($n = 8$ assays performed in duplicate), likely owing to its position at the TGEF1/Rac1 interface, as identified in the crystal structure (Table 2). K1431 lies at the interface between TGEF1 and Rac1 (Fig. 4B), suggesting that the

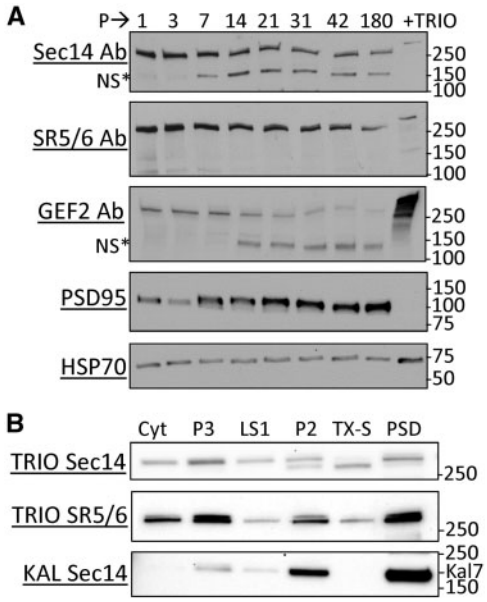

Figure 3. TRIO isoform expression in rodent brain. **(A)** Forebrain tissue was collected from male mice at various ages (p1–p180) and treated as described in Fig. 1B. Equal protein (30 μg) was loaded on each lane of an SDS polyacrylamide gradient gel. As a positive control, recombinant full length TRIO expressed in HEK293 cells was run on the same gel (+TRIO). (B) Adult male mouse forebrain extracts were subjected to subcellular fractionation as described in Miller *et al.* (67). Equal protein (20 μg) was loaded on each lane; similar results were seen in separate analyses of female mouse samples and validated with western blots for GM130, GAPDH, GluN2B, PSD95 and Kal7. The 165 kDa NS* non-specific band detected in (B) was shown to reside primarily in the lysed synaptosomal fraction (LS1).

K1431M mutation may reduce binding of TGEF1 to Rac1. The schizophrenia-associated F1538Intron construct (25), in which the second exon of the pleckstrin-homology (PH) domain is deleted and a 19-residue segment of the intron is translated, showed both the expected smaller protein and very low expression levels, suggesting that this mutant protein was unstable. Furthermore, despite its low level of expression, the activity of the TGEF1 F1538Intron variant was readily detectable and significantly above controls.

Full-length TRIO and TRIO8 are less active than TGEF1, and the K1431M mutation further reduces this activity

While the TGEF1 construct provided a useful screening background to test many TRIO sequence variants, testing the impact of the variants on GEF activity within the context of the native protein is essential (Fig. 5). However, it was not possible to achieve the same level of protein expression with the longer TRIO isoforms as with TRIO8 or TGEF1, owing to toxicity at higher levels of vector (Fig. 5B). As expected from previous work on KALIRIN (67,74) and *Drosophila* Trio (75), the larger TRIO proteins had reduced ability to activate Rac1 compared with TGEF1 alone (Fig. 5A). While TRIO9 is clearly the major isoform expressed in the human brain, the presence of a second GEF domain could complicate the analysis. To avoid this issue, we opted to evaluate the effect of TGEF1 mutations in TRIO8. When assessed in TRIO8, the K1431M mutation markedly reduced Rac1 activation (Fig. 5C), as it did in TGEF1 (Fig. 4D).

The low activity of the autism- and schizophrenia-associated TRIO variants (K1431M, F1538Intron) raised the possibility that a less active GEF could exert a dominant negative effect, interfering with Rac1 activation by a WT allele. To test this possibility, we performed mixing experiments by varying the amounts of vector to match the levels of protein expression (Fig. 5D). The lesser activities of the K1431M and F1538Intron variants were simply additive to WT TGEF1 activity, with no evidence of competition or a dominant negative effect. These data suggest that these disease-associated *de novo* variants act as hypomorphs.

A bipolar disorder-associated GEF2 variant yields increased activity, confirming a distinct mode of GEF2 regulation

To assess the impact of *de novo* mutations and rare sequence variants on TGEF2 activity (Fig. 6A), we established a quantitative cell-based biosensor assay for RhoA. The RhoA bioassay functions like the Rac1 bioassay, except RhoA activation induces a conformational change by binding to the Rho binding domain of PKN1, promoting FRET between CFP and YFP, leading to emission at 525 nm. As expected, transfection of increasing amounts of WT TGEF2 yielded a dose-dependent increase in RhoA biosensor FRET (Fig. 6B and C). As observed for a homologous RhoGEF, p63RhoGEF, the PH portion of TGEF2 exerts an inhibitory effect on the activity of the preceding DH domain (76–78). Based upon identified mRNAs that encode the Dbl-homology (DH) 2 domain of TRIO but lack the PH2 domain, a shorter TRIO GEF2 isoform (TDH2) was developed (Fig. 6A) (65). RhoA bioassays performed with TDH2 revealed that, as expected, TDH2 was a more active RhoA GEF than TGEF2, which includes the inhibitory PH2 domain (Fig. 6B and C).

The dose-dependent responses of the control D2113N variant and the case-related R2141W, D2144N and V2220G variants were indistinguishable from WT TGEF2 (Fig. 6C). When tested using the shorter TDH2 construct, the D2113N, R2141W and D2144N proteins did not differ from WT TDH2 (Fig. 6C). Strikingly, the bipolar disorder-associated M2145T variant in TGEF2 yielded consistently higher RhoA biosensor activity at all levels tested, compared with similar expression levels of WT TGEF2 (Fig. 6D and E). M2145 is located at the boundary of the DH2 and PH2 domains of TRIO, suggesting that the M2145T variant restricts the ability of the TRIO PH2 domain to inhibit the TRIO DH2 domain. The M2145T variant had no effect on TDH2 function (Fig. 6D and E), supporting the suggestion that M2145T restricts the ability of the PH2 domain to inhibit the DH2 domain in TGEF2 and supporting the model by which the PH2 domain negatively regulates TDH2 RhoA GEF activity.

Discussion

In this study, we confirmed that TRIO9, but not full length TRIO, is the major postnatal TRIO isoform in both human and mouse brain. TRIO9 is developmentally regulated, decreasing in expression after birth as previously observed (35,62,47,68–70). Furthermore, the *TRIO* gene was shown to have an enrichment of *de novo* mutations in neurodevelopmental disease in this study and previous studies (13,31,32) and a high number of rare sequence variants not observed in control individuals. Prediction algorithms, such as PolyPhen2 and Provean, suggested that many of these mutations and variants were damaging to protein function. We tested these predictions biochemically to identify mechanisms by which they could impact TRIO function, such as reduced expression levels or impaired activity. Owing to the low-throughput nature of these experiments, one limitation was an inability to test every mutation

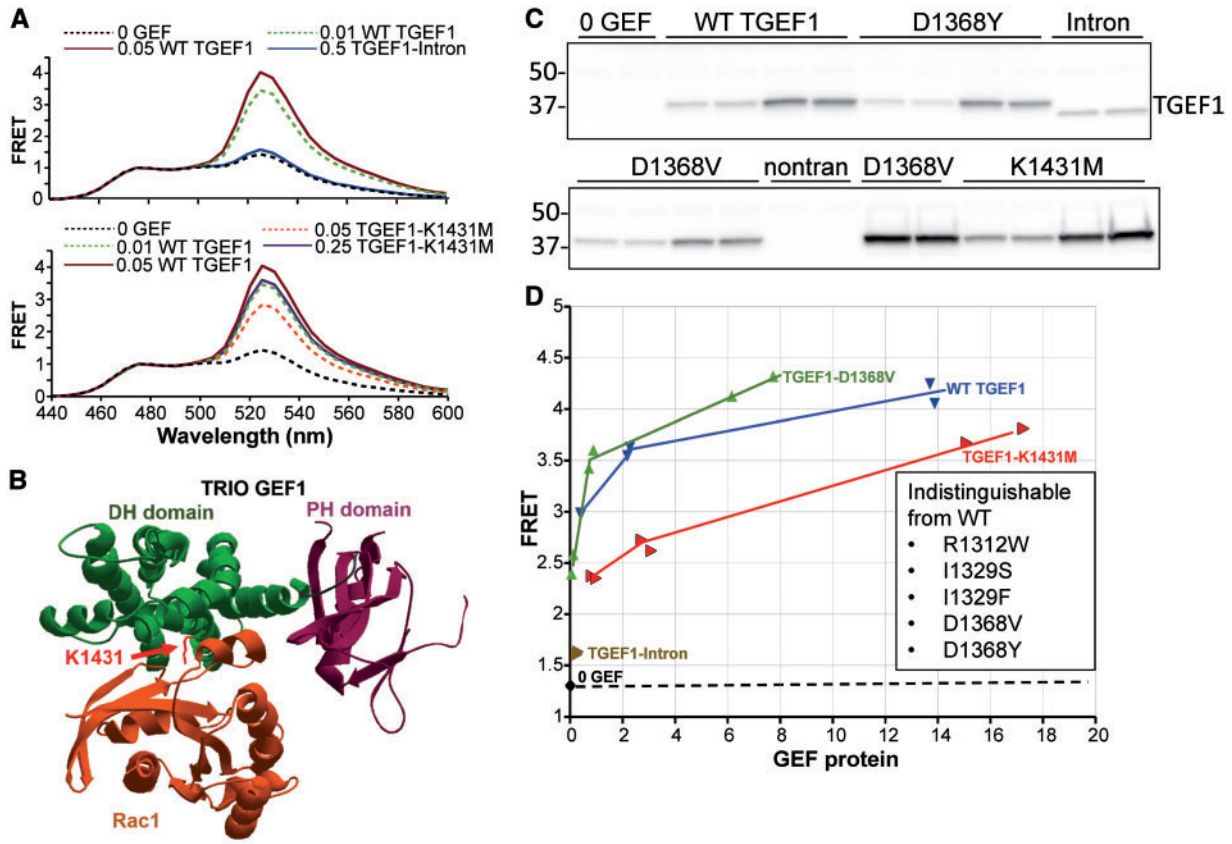

Figure 4. Rac1-activation assays: some TGEF1 variants have severely depressed activity. **(A)** Equal amounts of Rac1 FRET biosensor vector and varying amounts of GEF vector were transfected into paired wells of HEK293 cells; the numbers in the labels indicate μg of vector per well. After 30 h, the FRET signal was determined for each well, cells were extracted and the level of GEF expression in each well was determined by Western analysis. Rac1-biosensor assays using HEK293 cells demonstrated that the K1431M variant was substantially less potent than WT TGEF1, while the F1538Intron variant (truncated halfway through PH1) was almost inactive. **(B)** Diagram of TRIO GEF1 (DH domain in green/PH domain in purple) in complex with Rac1 (orange) from the Protein Data Bank (www.rcsb.org: crystals: 2NZ8 with Rac1, 1NTY without Rac1). The K1431 position is at the TGEF1/Rac1 interface. **(C)** Quantitative immunoblot analysis of GEF proteins expressed in the Rac1 biosensor assay. Vector amounts ranged from 0.01 to 0.20 μg for most constructs, up to 0.50 μg for the F1538Intron construct. **(D)** FRET signal plotted against relative GEF protein expression (C) determined by immunoblot. On average, the K1431M variant was 8% as active as WT TGEF1, while 5 mutants were as active as WT: R1312W, I1329S, I1329F, D1368V and D1368Y. The F1538Intron variant was <2% as active as WT and was expressed very poorly. All constructs were tested in duplicate in five to eight assays with similar results.

and variant, forcing us to prioritize and only study those that were most likely to impact function based upon algorithmic and structure-based predictions. We discovered that one autism-associated *de novo* mutation in TGEF1 (K1431M) decreased its activity toward Rac1, likely through impaired TRIO/Rac1 interactions. In contrast, a schizophrenia-associated rare sequence variant (aberrant splicing) in TGEF1 (F1538Intron) was substantially less active, when normalized to protein level, and expressed very poorly, suggesting protein instability. A recent study examined a different mutation that deleted almost all of the PH1 domains in three related patients and, using a Rac-pulldown activation assay, found that TGEF1 activity was reduced (30). Since half of the affected individuals in this previous study also have a 15q11.2 microdeletion, it is not clear that the loss of *TRIO* PH1 was the cause of the intellectual disability and microcephaly (30). Three additional variants studied exhibit an autosomal dominant inheritance pattern (30); however, our mixing experiments strongly suggest that the disease-related *TRIO* variants lead to haploinsufficiency. We propose that these three variants (30) may also be examples of haploinsufficient alleles, which would exhibit the same inheritance pattern as an autosomal dominant allele.

The situation for TGEF2 is quite different, since the natural splice variant TDH2, which lacks the PH2 domain entirely, is far more active than the larger TGEF2 protein in the RhoA activation assay. Analyzing genetic damage to the TGEF2 domain, one bipolar disorder-associated rare variant (M2145T) impaired TRIO regulation. In particular, M2145T appeared to restrict the ability of the TPH2 domain to negatively regulate the RhoA GEF activity of the TDH2 domain. Overall, this study suggests that neurodevelopmental disease-associated genetic damage may impact the TGEF1 and TGEF2 domains through loss-of-function and gain-of-function mutations/variants, respectively.

Use of algorithms to predict impact of sequence variation on protein function

Of further interest, many of the tested mutations/variants that were predicted to be damaging had no measurable effect on TRIO protein expression or GEF function. Table 3 lists the variants tested in this study and a few selected others. For each, the PolyPhen2 and Provean predictions for damage to the protein structure and function are provided. In general, the predictions

Table 3. Summary of GDP/GTP exchange factor *de novo* mutants and rare variants in TRIO

De novo mutation or variant position	TRIO protein domain	Disease source	PolyPhen2 prediction	Provean prediction	Clustal substitutes	Region crystal structure	Enzyme activity
R1276X	Before GEF1	Schizophrenia[a]	n/a	n/a	n/a	n/a	Dead (0 GEF)
R1312W	GEF1	Autism (22)	1.000	−3.7	H, L, Y, N	α-Helix	Normal
I1329F; S	GEF1	Control (F; S)	0.997;0.999	−3.3;−4.7	M, L, F	Loop	Normal (F; S)
I1329 frameshift	GEF1	Autism (25)	n/a	n/a	n/a	n/a	Dead (0 GEF)
D1368V; Y	GEF1	Intellectual Disability (V) (26); Control (Y)	0.984;1.000	−7.2	L, R, S	loop	Normal (V; Y)
K1431M	**GEF1**	**Autism** (23)	**1.000**	**−5.0**	**R**	**GEF1/Rac1 interface**	**8% active**
L1439M	GEF1	Schizophrenia (56)	0.999	−1.8	M, Y	α-Helix	Not tested
S1459G	GEF1	Schizophrenia (56)	0.999	−2.8	G, D, R, T, K	α-Helix	Not tested
F1538 Intron	**Aberrant splicing in PH1 to stop**	**Schizophrenia** (56)	n/a	**−13.2**	**Removes PH1 C-terminus**	n/a	**<2% active**
K1918X	Before GEF2	Schizophrenia[a]	n/a	n/a	n/a	n/a	Dead (0 GEF)
R2086C	GEF2	Control (56)	0.32	−0.67	E, K, Q	α-Helix	Not tested
D2113N	GEF2	Control (56)	0.996	−3.3	E	α-Helix	Normal
K2119E	GEF2	Control[b]	0.19	0.80	E, N	Loop	Not tested
R2141W; Q	GEF2	Control (W);Bipolar disorder (Q) (56)	1.000	−4.3	S	α-Helix	Normal (W); Not tested (Q)
D2144N	GEF2	Schizophrenia (56)	0.998	−3.9	None	α-Helix	Normal
M2145T	**GEF2**	**Bipolar disorder** (56)	**0.952**	**−4.6**	**S**	**α-Helix; DH-PH border**	**~400% Active**
V2220G; L	GEF2	Control (G);Autism (L) (25)	0.995;0.001	−4.0; −0.69	M	Loop	Normal (G); Not tested (L)

The subset of variants tested (numbered using NM_007118) with the source of each mutation identified. For each variant, structural predictions using PolyPhen2 (http://genetics.bwh.harvard.edu/pph2/) and Provean (http://sift.jcvi.org/) are shown, along with alternative residues uncovered in a limited Clustal alignment (http://www.ebi.ac.uk/Tools/msa/clustalo/). PolyPhen2 scores range from 0 to 1.000, with 0 being the most benign and 1.000 signifying changes expected to be the most damaging. Provean numbers cover a much wider range, with −2.50 and more negative expected to be progressively more damaging, and numbers closer to zero and positive expected to be more benign. For TGEF1, the Clustal included KALRN (NP_001019831.2), DBS (XP_011535788.2), DBL (NP_001165347.1), FGD1 (AAA57004.1) and TIAM1 (AAA98443.1). For TGEF2, the Clustal included KALRN, DDL and P63RHOGEF (NP_891992.2). The structural predictions were from the Protein Data Bank (http://www.rcsb.org/pdb) using the structure of TGEF1 complexed with RAC1 (2NZ8) and P63RHOGEF with RHOA and Gαq (2RGN).

[a]A personal communication with Daniel Howrigan and Benjamin Neale (Broad Institute of MIT and Harvard: Boston, MA, USA).

[b]The ExAc Browser as the reference. X, stop/termination codon; GEF, guanine nucleotide exchange factor; PH, pleckstrin homology domain; DH, Dbl homology domain.

identified more mutations/variants as damaging than observed when testing the expression and activity of the isolated GEF domains; the Provean predictions aligned more closely with our data than the PolyPhen2 predictions. In contrast, the Clustal predictions were very instructive; in most cases, if several residues were tolerated at a chosen position, looking across species at similar GEFs, there was a reasonable possibility that the variant would be fully active. If the variation identified by Clustal was only within class (e.g. positively charged K ↔ R), then a change that was 'out of class' was considered more likely to be deleterious. Similarly, known crystal structures were extremely predictive. For TGEF1, only 1 variant (K1431M; 'out of class') was at a position that could clearly be important, namely the TGEF1/Rac1 interface, and the change (K → M) resulted in a similarly large but uncharged residue replacing the positively charged lysine. For TGEF2, the crystal was less predictive, as only a closely related structure was available (not the TGEF2 structure). However, the substitution (M2145T; 'out of class') at the DH2–PH2 boundary would be a logical place for an effect, given the strong inhibition of PH2 on the activity of DH2 (76–78).

Model for regulation of neurite outgrowth by TRIO GEF1 and GEF2 domains

Based on these data, we propose a model by which TGEF1 is natively active and signals through Rac1 to promote dendritic initiation and branching; thus loss-of-function mutations in TGEF1 impair proper nervous system development. On the other hand, TGEF2 is natively inhibited, and signals through RhoA to negatively regulate dendritic initiation and branching, such that gain-of-function mutations in TGEF2 impair proper nervous system development. The inclusion of both the GEF1 and GEF2 domains in the same TRIO protein isoform allows for both modules to be physically coupled into an easy 'switch' from dendritic stability to instability when needed. As a next step, the impact of the TRIO K1431M, F1538Intron and M2145T mutations on neurite outgrowth, dendrite arborization and dendritic spine density can be directly assessed by knockdown/rescue experiments in primary neuronal culture. Overall, by understanding this and other molecular pathways underlying neurodevelopmental disorders, treatments targeted at correcting disease mechanisms may be developed in the future.

Materials and Methods

Targeted search for *de novo* mutation and rare sequence variants in *TRIO*

A targeted search of triad exomes was performed of published and unpublished studies of neurodevelopmental disorders, including epileptic encephalopathy (28), intellectual disability (26,27), autism spectrum disorders (23–25,57–59) and schizophrenia (12,17,19–21,55) (D. Howrigan and B. Neale, personal

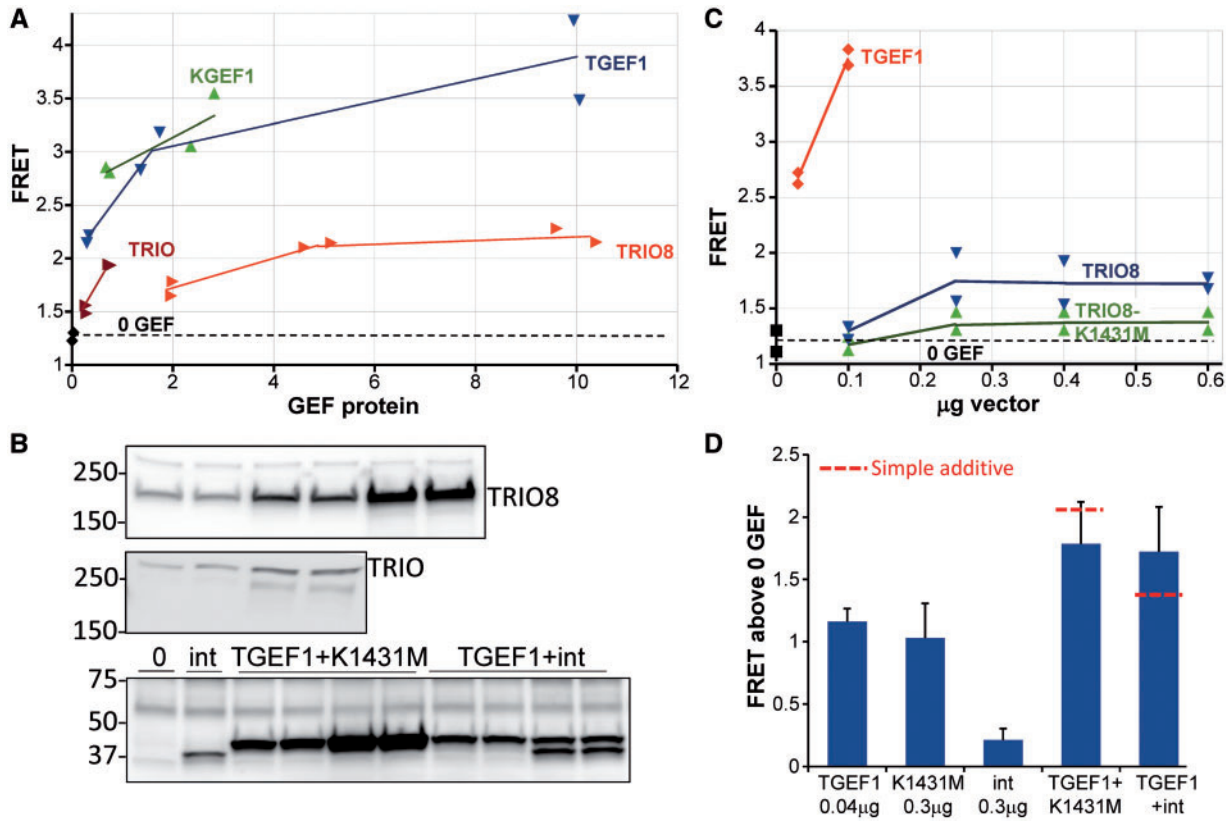

Figure 5. Disease-associated allele inhibits GEF1 function in larger TRIO isoforms. **(A)** FRET signal plotted against relative Western signal for TRIO GEF1 (TGEF1), rat Kalirin GEF1 (KGEF1), full-length TRIO and TRIO8. TGEF1, KGEF1 and full-length TRIO were detected with Myc monoclonal antibody, while TRIO8 and full-length TRIO were detected with TRIO Sec14 antibody; full-length TRIO was used to normalize signal obtained with these two antibodies. Results typify five similar assays in duplicate. **(B)** Immunoblots for TRIO8 (0.05–0.50 µg vector) and for full-length TRIO (0.15–0.50 µg vector; 4.6-fold longer exposure than for TRIO8) are shown, along with a mixing experiment using 0.3 µg vector for F1538Intron or K1431M with 0.04 µg vector for WT TGEF1. **(C)** An example of 3 similar assays showing that TRIO8-K1431M was significantly less active than TRIO8, as also found with the TGEF1 constructs (Fig. 4). **(D)** Additivity/interference test: assays performed separately and pairwise with WT TGEF1, TGEF1-K1431M and TGEF1-F1538Intron show additivity, not interference, when mixing active and less active constructs (representative of two assays).

communication). Based on the mutation model expectation derived in Samocha *et al.* (60), we calculated the expected number of missense or protein-truncating mutations in *TRIO* under a null model of no association. Using a Poisson distributed model, the probability of observing the actual number of mutations was calculated and corrected for the total number of tests across the exome (exome-wide significance threshold $= 1 \times 10^{-6}$). To determine if the *de novo* mutations were observed in the normal population, they were compared with controls in the Exome Aggregation Consortium (ExAc) database (http://exac.broadinstitute.org/, accessed on December 1, 2015). Rare *TRIO* sequence variants in schizophrenia and bipolar disorder were identified by comparing data from Genovese *et al.* (56) to control individuals in the ExAc database (http://exac.broadinstitute.org/, accessed on December 1, 2015).

Biosensor assays

The Rac1 biosensor assays using HEK293 cells have been described (73). The RhoA biosensor developed by van Unen *et al.* (79) had the same spectral characteristics as the Rac1 biosensor and RhoA assays were also carried out using transiently transfected HEK293 cells. Western blot analyses were performed with rabbit TRIO Sec14 antibody [CT233 (34)] or with a Myc monoclonal antibody [clone 9E10 (80)]. Western blots were quantified from non-saturated images using GeneTools from SynGene (67); all wells of HEK293 cells were transfected with a constant amount of Rac1 or RhoA biosensor.

Quantitative polymerase chain reaction

Using fetal and adult human RNA from Clontech and BioChain, random primed cDNA was prepared using the BioRad iScript kit as described (67). qPCR was performed using the primers listed in Table 2; all products were 120–130 bp and all primers had calculated melting temperatures of 60–62 °C. TRIO products were normalized to the GAPDH internal standard, yielding consistent data across eight assays and between commercial sources.

TRIO vector constructs and variants

The vector encoding full-length myc-His-TRIO was described previously and was based on the U42390.1 (short front) sequence (34). A cDNA encoding TRIO8 was made by PCR amplification of the Exon 36a unique COOH-terminal extension described in Mc Pherson *et al.* (34) and in 16 TRIO transcripts in Tilgner *et al.* (65) (HYVDLCSVSVLAQFPYLSV*); the vector encoding TRIO8 included the 59 additional NH_2-terminal residues present in NM_007118 (long front) and did not include an epitope tag. The unique NH_2-terminal in the TDH2 construct was identified as Exon 34a in McPherson *et al.* (34) and was identified in 6 transcripts in Tilgner *et al.* (65) (MPNGLKPVDTLDSLSSVSSAYCSGGQPGTCKYWILDLD).

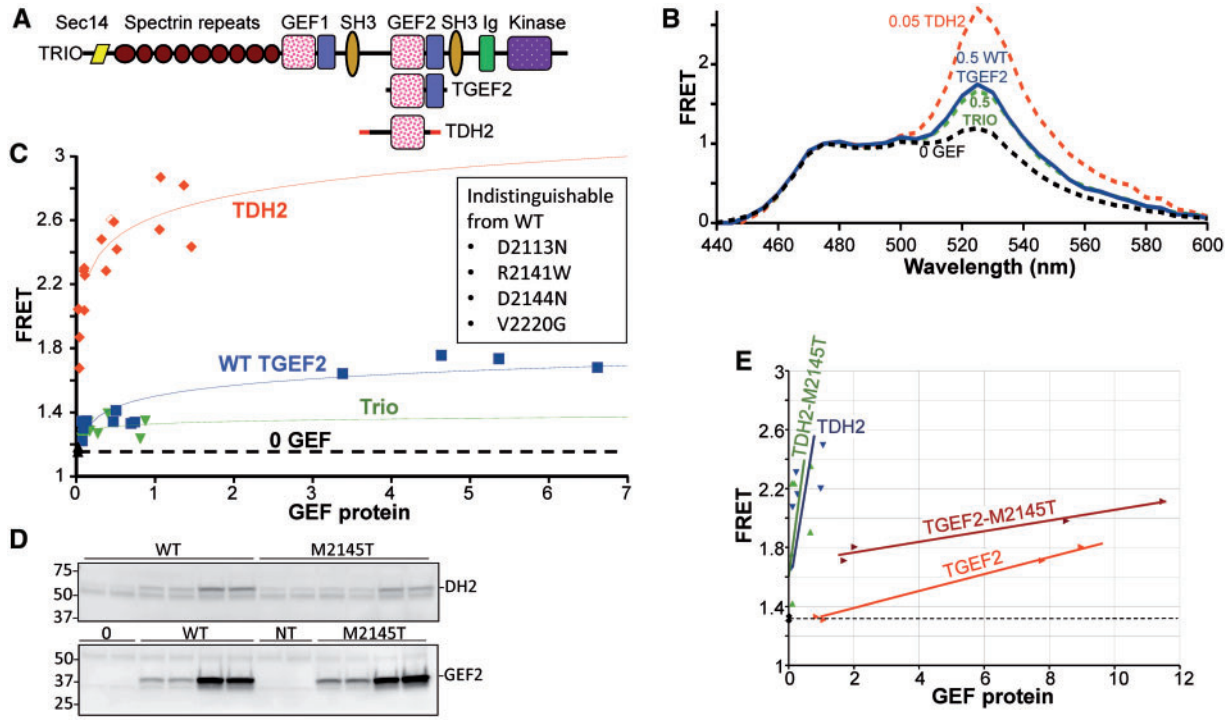

Figure 6. RhoA-activation assays: one TGEF2 variant has markedly augmented activity. **(A)** In addition to full-length TRIO and TGEF2, TDH2, a naturally occurring isoform that lacks a PH domain, was tested. **(B)** FRET spectra for the various constructs (averages of duplicates), showing comparable activity for TGEF2 and TRIO with 0.5 μg vector and far more activity for TDH2 with 0.05 μg vector. **(C)** Composite data from two assays comparing RhoA activation by TDH2, TGEF2 and TRIO (all Myc-tagged; representative of four assays). Lines are best-fit logarithmic fits created using Open Office. **(D)** Immunoblots for TDH2 and TGEF2, WT and M2145T. Vector amounts ranged from 0.01–0.20 μg for TDH2 to 0.20–0.50 μg for TGEF2. **(E)** The TGEF2-M2145T construct was about ×4 as active as WT TGEF2, while in the TDH2 backbone the M2145T mutation was without effect in four assays. In both TDH2 and TGEF2, four mutations were without effect in four to five assays: D2113N, R2141W, D2144N and V2220G.

The unique COOH-terminal of TDH2 is the extension of Exon 45 into Intron 45 (VMRLLFFKRAPLPSSLSFVLDYFSPHRES*) as identified in 6 transcripts in Tilgner *et al.* (65). The full-length TDH2 construct was constructed with a Myc epitope at the NH_2-terminal by PCR from fetal human RNA from BioChain. The TGEF1-F1538Intron construct, which includes Exon 30, the first of the 2 exons comprising the PH1 domain, then extending into Intron 30, was constructed by PCR to create a COOH-terminal that matched ENST00000509967. Site-directed variants were introduced by mutagenesis with the QuikChange kit (Stratagene); to avoid confusion with the literature, residues are always numbered as for NM_007118 (long front). Subtracting 59 converts NM_007118 amino acid numbers to U42390.1 amino acid numbers, the reference standard used in the Protein Data Bank crystal structures. All constructs were verified by DNA sequencing.

Immunoblotting and *Trio*$^{fl/fl}$ mice

Protein concentrations were determined by BCA Assay (Pierce). Protein amounts loaded are provided in Figure legends. The TRIO Kinase domain antibody was raised by immunization of rabbits (Pocono Rabbit Farm and Laboratory, Canadensis, PA, USA) with the purified products from pMAL–MBP fusion with amino acids 2796–3053 of TRIO (NP_009049) and affinity purified on resin with MBP alone first and then the same bacterial MBP–TRIO protein (81). TRIO GEF2 (DH2) antibody was raised by immunization of rabbits (Pocono Rabbit Farm and Laboratory) with the purified products from pGEX6P1 fusion with amino acids 1968–2158 of TRIO (NP_009049) and affinity purified on resin with GST first (to remove GST binding) and then the same bacterial GST-TRIO protein (81). TRIO Sec14 antibody was raised by immunization of rabbits (Covance Research Products, Denver, PA, USA) with the cleaved, purified product from a pGEX6P1 fusion with amino acids 1–234 of TRIO (NP_009049) and affinity purified on resin with the same recombinant protein (82). The KALIRIN Sec14 (82), TRIO SR5/6 and TRIO Kinase (C-terminal peptide) (34) antibodies were described previously. The PSD95 (Neuromab 75-028) and HSP70 (Santa Cruz, SC 32239) antibodies are commercial monoclonal mouse antibodies. To test the validity of the new TRIO antisera, conditional TRIO knockout mice (62,63) were crossed with *NEX-Cre* mice under the *Neurod6* promoter (64), and cortical extracts were subjected to western analysis.

Acknowledgements

We thank Andrew Yanik, Taylor Larese and Yanping Wang for tireless support during this work. We particularly appreciate the personal communication of unpublished, Taiwanese exome-sequenced *de novo* mutations in schizophrenia from Daniel Howrigan and Benjamin Neale (Broad Institute of MIT and Harvard: Boston, MA, USA).

Conflict of Interest statement. None declared.

Funding

This work was supported by National Institutes of Health Grants DK032948 (R.E.M., B.A.E.), NS089662 (A.J.K.) and GM117061 (Y.I.W.), a grant from the Stanley Center for Psychiatric Research

(A.J.K., B.A.E., R.E.M.) and the Daniel G. Schwartzberg Fund (B.A.E., R.E.M.).

References

1. Kessler, R.C., Chiu, W.T., Demler, O., Merikangas, K.R. and Walters, E.E. (2005) Prevalence, severity, and comorbidity of 12-month DSM-IV disorders in the National Comorbidity Survey Replication. *Arch. Gen. Psychiatry*, **62**, 617–627.
2. Regier, D.A., Narrow, W.E., Rae, D.S., Manderscheid, R.W., Locke, B.Z. and Goodwin, F.K. (1993) The de facto US mental and addictive disorders service system. Epidemiologic catchment area prospective 1-year prevalence rates of disorders and services. *Arch. Gen. Psychiatry*, **50**, 85–94.
3. Developmental Disabilities Monitoring Network Surveillance Year 2010 Principal Investigators and Centers for Disease Control and Prevention (CDC) (2014) Prevalence of autism spectrum disorder among children aged 8 years - autism and developmental disabilities monitoring network, 11 sites, United States, 2010. *MMWR. Surveill. Summ.*, **63**, 1–21.
4. Maulik, P.K., Mascarenhas, M.N., Mathers, C.D., Dua, T. and Saxena, S. (2011) Prevalence of intellectual disability: a meta-analysis of population-based studies. *Res. Dev. Disabil.*, **32**, 419–436.
5. Fusar-Poli, P., Papanastasiou, E., Stahl, D., Rocchetti, M., Carpenter, W., Shergill, S. and McGuire, P. (2015) Treatments of negative symptoms in schizophrenia: meta-analysis of 168 randomized placebo-controlled trials. *Schizophr. Bull.*, **41**, 892–899.
6. Lindström, L., Lindström, E., Nilsson, M. and Höistad, M. (2017) Maintenance therapy with second generation antipsychotics for bipolar disorder—a systematic review and meta-analysis. *J. Affect. Disord.*, **213**, 138–150.
7. Myers, S.M. and Johnson, C.P. (2007) Management of children with autism spectrum disorders. *Pediatrics*, **120**, 1162–1182.
8. Konopaske, G.T., Lange, N., Coyle, J.T. and Benes, F.M. (2014) Prefrontal cortical dendritic spine pathology in schizophrenia and bipolar disorder. *JAMA Psychiatry*, **71**, 1323–1331.
9. Glantz, L.A. and Lewis, D.A. (2000) Decreased dendritic spine density on prefrontal cortical pyramidal neurons in schizophrenia. *Arch. Gen. Psychiatry*, **57**, 65–73.
10. Hutsler, J.J. and Zhang, H. (2010) Increased dendritic spine densities on cortical projection neurons in autism spectrum disorders. *Brain Res.*, **1309**, 83–94.
11. von Bohlen Und Halbach, O. (2010) Dendritic spine abnormalities in mental retardation. *Cell Tissue Res.*, **342**, 317–323.
12. Fromer, M., Pocklington, A.J., Kavanagh, D.H., Williams, H.J., Dwyer, S., Gormley, P., Georgieva, L., Rees, E., Palta, P. and Ruderfer, D.M. (2014) De novo mutations in schizophrenia implicate synaptic networks. *Nature*, **506**, 179–184.
13. Jiang, Y., Han, Y., Petrovski, S., Owzar, K., Goldstein, D.B. and Allen, A.S. (2015) Incorporating functional information in tests of excess de novo mutational load. *Am. J. Hum. Genet.*, **97**, 272–283.
14. Penzes, P., Cahill, M.E., Jones, K.A., VanLeeuwen, J.-E. and Woolfrey, K.M. (2011) Dendritic spine pathology in neuropsychiatric disorders. *Nat. Neurosci.*, **14**, 285–293.
15. Lee, S.H., Ripke, S., Neale, B.M., Faraone, S.V., Purcell, S.M., Perlis, R.H., Mowry, B.J., Thapar, A., Goddard, M.E. and Witte, J.S. (2013) Genetic relationship between five psychiatric disorders estimated from genome-wide SNPs. *Nat. Genet.*, **45**, 984–994.
16. Zhou, Y., Kaiser, T., Monteiro, P., Zhang, X., Van der Goes, M.S., Wang, D., Barak, B., Zeng, M., Li, C., Lu, C. *et al.* (2016) Mice with Shank3 mutations associated with ASD and schizophrenia display both shared and distinct defects. *Neuron*, **89**, 147–162.
17. McCarthy, S.E., Gillis, J., Kramer, M., Lihm, J., Yoon, S., Berstein, Y., Mistry, M., Pavlidis, P., Solomon, R., Ghiban, E. *et al.* (2014) De novo mutations in schizophrenia implicate chromatin remodeling and support a genetic overlap with autism and intellectual disability. *Mol. Psychiatry*, **19**, 652–658.
18. Craddock, N., Owen, M.J. (2010) The Kraepelinian dichotomy—going, going... but still not gone. *Br. J. Psychiatry*, **196**, 92–95.
19. Girard, S.L., Gauthier, J., Noreau, A., Xiong, L., Zhou, S., Jouan, L., Dionne-Laporte, A., Spiegelman, D., Henrion, E., Diallo, O. *et al.* (2011) Increased exonic de novo mutation rate in individuals with schizophrenia. *Nat. Genet.*, **43**, 860–863.
20. Xu, B., Ionita-Laza, I., Roos, J.L., Boone, B., Woodrick, S., Sun, Y., Levy, S., Gogos, J.A. and Karayiorgou, M. (2012) De novo gene mutations highlight patterns of genetic and neural complexity in schizophrenia. *Nat. Genet.*, **44**, 1365–1369.
21. Gulsuner, S., Walsh, T., Watts, A.C., Lee, M.K., Thornton, A.M., Casadei, S., Rippey, C., Shahin, H., Nimgaonkar, V.L., Go, R.C.P. *et al.* (2013) Spatial and temporal mapping of de novo mutations in schizophrenia to a fetal prefrontal cortical network. *Cell*, **154**, 518–529.
22. O'Roak, B.J., Vives, L., Fu, W., Egertson, J.D., Stanaway, I.B., Phelps, I.G., Carvill, G., Kumar, A., Lee, C., Ankenman, K. *et al.* (2012) Multiplex targeted sequencing identifies recurrently mutated genes in autism spectrum disorders. *Science*, **338**, 1619–1622.
23. Sanders, S.J., Murtha, M.T., Gupta, A.R., Murdoch, J.D., Raubeson, M.J., Willsey, A.J., Ercan-Sencicek, A.G., DiLullo, N.M., Parikshak, N.N., Stein, J.L. *et al.* (2012) De novo mutations revealed by whole-exome sequencing are strongly associated with autism. *Nature*, **485**, 237–241.
24. Iossifov, I., O'Roak, B.J., Sanders, S.J., Ronemus, M., Krumm, N., Levy, D., Stessman, H.A., Witherspoon, K.T., Vives, L., Patterson, K.E. *et al.* (2014) The contribution of de novo coding mutations to autism spectrum disorder. *Nature*, **515**, 216–221.
25. De Rubeis, S., He, X., Goldberg, A.P., Poultney, C.S., Samocha, K., Cicek, A.E., Kou, Y., Liu, L., Fromer, M., Walker, S. *et al.* (2014) Synaptic, transcriptional and chromatin genes disrupted in autism. *Nature*, **515**, 209–215.
26. de Ligt, J., Willemsen, M.H., van Bon, B.W.M., Kleefstra, T., Yntema, H.G., Kroes, T., Vulto-van Silfhout, A.T., Koolen, D.A., de Vries, P., Gilissen, C. *et al.* (2012) Diagnostic exome sequencing in persons with severe intellectual disability. *N. Engl. J. Med.*, **367**, 1921–1929.
27. Rauch, A., Wieczorek, D., Graf, E., Wieland, T., Endele, S., Schwarzmayr, T., Albrecht, B., Bartholdi, D., Beygo, J., Di Donato, N. *et al.* (2012) Range of genetic mutations associated with severe non-syndromic sporadic intellectual disability: an exome sequencing study. *Lancet*, **380**, 1674–1682.
28. EuroEPINOMICS-RES Consortium, Epilepsy Phenome/Genome Project and Epi4K Consortium (2014) De novo mutations in synaptic transmission genes including DNM1 cause epileptic encephalopathies. *Am. J. Hum. Genet.*, **95**, 360–370.
29. Ba, W., Yan, Y., Reijnders, M.R.F., Schuurs-Hoeijmakers, J.H.M., Feenstra, I., Bongers, E.M.H.F., Bosch, D.G.M., De Leeuw, N., Pfundt, R., Gilissen, C. *et al.* (2016) TRIO loss of function is associated with mild intellectual disability and affects dendritic branching and synapse function. *Hum. Mol. Genet.*, **25**, 892–902.

30. Pengelly, R.J., Greville-Heygate, S., Schmidt, S., Seaby, E.G., Jabalameli, M.R., Mehta, S.G., Parker, M.J., Goudie, D., Fagotto-Kaufmann, C., Mercer, C. *et al.* (2016) Mutations specific to the Rac-GEF domain of TRIO cause intellectual disability and microcephaly. *J. Med. Genet.*, **53**, 735–742.
31. Deciphering Developmental Disorders Study (2015) Large-scale discovery of novel genetic causes of developmental disorders. *Nature*, **519**, 223–228.
32. Deciphering Developmental Disorders Study (2017) Prevalence and architecture of de novo mutations in developmental disorders. *Nature*, **542**, 433–438.
33. Debant, A., Serra-Pages, C., Seipel, K., O'Brien, S., Tang, M., Park, S.H. and Streuli, M. (1996) The multidomain protein Trio binds the LAR transmembrane tyrosine phosphatase, contains a protein kinase domain, and has separate rac-specific and rho-specific guanine nucleotide exchange factor domains. *Proc. Natl. Acad. Sci. U.S.A.*, **93**, 5466–5471.
34. McPherson, C.E., Eipper, B.A. and Mains, R.E. (2005) Multiple novel isoforms of Trio are expressed in the developing rat brain. *Gene*, **347**, 125–135.
35. Portales-Casamar, E., Briançon-Marjollet, A., Fromont, S., Triboulet, R. and Debant, A. (2006) Identification of novel neuronal isoforms of the Rho-GEF Trio. *Biol. Cell*, **98**, 183–193.
36. Yoshizuka, N., Moriuchi, R., Mori, T., Yamada, K., Hasegawa, S., Maeda, T., Shimada, T., Yamada, Y., Kamihira, S. and Tomonaga, M. (2004) An alternative transcript derived from the trio locus encodes a guanosine nucleotide exchange factor with mouse cell-transforming potential. *J. Biol. Chem.*, **279**, 43998–44004.
37. Schmidt, S. and Debant, A. (2014) Function and regulation of the Rho guanine nucleotide exchange factor Trio. *Small GTPases*, **5**, e29769.
38. van Rijssel, J. and van Buul, J.D. (2012) The many faces of the guanine-nucleotide exchange factor trio. *Cell Adh. Migr.*, **6**, 482–487.
39. Blangy, A., Vignal, E., Schmidt, S., Debant, A., Gauthier-Rouvière, C. and Fort, P. (2000) TrioGEF1 controls Rac- and Cdc42-dependent cell structures through the direct activation of rhoG. *J. Cell Sci.*, **113**, 729–739.
40. Bellanger, J.M., Lazaro, J.B., Diriong, S., Fernandez, A., Lamb, N. and Debant, A. (1998) The two guanine nucleotide exchange factor domains of Trio link the Rac1 and the RhoA pathways in vivo. *Oncogene*, **16**, 147–152.
41. Seipel, K., Medley, Q.G., Kedersha, N.L., Zhang, X.A., O'Brien, S.P., Serra-Pages, C., Hemler, M.E. and Streuli, M. (1999) Trio amino-terminal guanine nucleotide exchange factor domain expression promotes actin cytoskeleton reorganization, cell migration and anchorage-independent cell growth. *J. Cell Sci.*, **112**, 1825–1834.
42. Medley, Q.G., Buchbinder, E.G., Tachibana, K., Ngo, H., Serra-Pagès, C. and Streuli, M. (2003) Signaling between focal adhesion kinase and Trio. *J. Biol. Chem.*, **278**, 13265–13270.
43. Saito, K., Tautz, L. and Mustelin, T. (2007) The lipid-binding SEC14 domain. *Biochim. Biophys. Acta*, **1771**, 719–726.
44. Medley, Q.G., Serra-Pagès, C., Iannotti, E., Seipel, K., Tang, M., O'Brien, S.P. and Streuli, M. (2000) The Trio guanine nucleotide exchange factor is a RhoA target: binding of RhoA to the Trio immunoglobulin-like domain. *J. Biol. Chem.*, **275**, 36116–36123.
45. Iyer, S.C., Wang, D., Iyer, E.P.R., Trunnell, S.A., Meduri, R., Shinwari, R., Sulkowski, M.J., Cox, D.N. and Hassan, B.A. (2012) The RhoGEF trio functions in sculpting class specific dendrite morphogenesis in Drosophila sensory neurons. *PLoS One*, **7**, e33634.
46. Shivalkar, M. and Giniger, E. (2012) Control of dendritic morphogenesis by Trio in Drosophila melanogaster. *PLoS One*, **7**, e33737.
47. Miller, M.B., Yan, Y., Eipper, B.A. and Mains, R.E. (2013) Neuronal Rho GEFs in synaptic physiology and behavior. *Neuroscientist*, **19**, 255–273.
48. Xie, Z., Cahill, M.E. and Penzes, P. (2010) Kalirin loss results in cortical morphological alterations. *Mol. Cell. Neurosci.*, **43**, 81–89.
49. Cahill, M.E., Xie, Z., Day, M., Photowala, H., Barbolina, M.V., Miller, C.A., Weiss, C., Radulovic, J., Sweatt, J.D. and Disterhoft, J.F. (2009) Kalirin regulates cortical spine morphogenesis and disease-related behavioral phenotypes. *Proc. Natl. Acad. Sci. U.S.A.*, **106**, 13058–13063.
50. Penzes, P., Johnson, R.C., Kambampati, V., Mains, R.E. and Eipper, B.A. (2001) Distinct roles for the two Rho GDP/GTP exchange factor domains of kalirin in regulation of neurite growth and neuronal morphology. *J. Neurosci.*, **21**, 8426–8434.
51. Backer, S., Hidalgo-Sánchez, M., Offner, N., Portales-Casamar, E., Debant, A., Fort, P., Gauthier-Rouvière, C. and Bloch-Gallego, E. (2007) Trio controls the mature organization of neuronal clusters in the hindbrain. *J. Neurosci.*, **27**, 10323–10332.
52. Ma, X.-M., Kiraly, D.D., Gaier, E.D., Wang, Y., Kim, E.-J., Levine, E.S., Eipper, B.A. and Mains, R.E. (2008) Kalirin-7 is required for synaptic structure and function. *J. Neurosci.*, **28**, 12368–12382.
53. Kiraly, D.D., Stone, K.L., Colangelo, C.M., Abbott, T., Wang, Y., Mains, R.E. and Eipper, B.A. (2011) Identification of kalirin-7 as a potential post-synaptic density signaling hub. *J. Proteome Res.*, **10**, 2828–2841.
54. Ma, X.-M., Miller, M.B., Vishwanatha, K.S., Gross, M.J., Wang, Y., Abbott, T., Lam, T.T., Mains, R.E. and Eipper, B.A. (2014) Nonenzymatic domains of Kalirin7 contribute to spine morphogenesis through interactions with phosphoinositides and Abl. *Mol. Biol. Cell*, **25**, 1458–1471.
55. Xu, B., Roos, J.L., Dexheimer, P., Boone, B., Plummer, B., Levy, S., Gogos, J.A. and Karayiorgou, M. (2011) Exome sequencing supports a de novo mutational paradigm for schizophrenia. *Nat. Genet.*, **43**, 864–868.
56. Genovese, G., Fromer, M., Stahl, E.A., Ruderfer, D.M., Chambert, K., Landén, M., Moran, J.L., Purcell, S.M., Sklar, P., Sullivan, P.F., Hultman, C.M. and McCarroll, S.A. (2016) Increased burden of ultra-rare protein-altering variants among 4, 877 individuals with schizophrenia. *Nat. Neurosci.*, **19**, 1433–1441.
57. Neale, B.M., Kou, Y., Liu, L., Ma'ayan, A., Samocha, K.E., Sabo, A., Lin, C.-F., Stevens, C., Wang, L.-S., Makarov, V. *et al.* (2012) Patterns and rates of exonic de novo mutations in autism spectrum disorders. *Nature*, **485**, 242–245.
58. O'Roak, B.J., Vives, L., Girirajan, S., Karakoc, E., Krumm, N., Coe, B.P., Levy, R., Ko, A., Lee, C., Smith, J.D. *et al.* (2012) Sporadic autism exomes reveal a highly interconnected protein network of de novo mutations. *Nature*, **485**, 246–250.
59. Iossifov, I., Ronemus, M., Levy, D., Wang, Z., Hakker, I., Yamrom, B., Lee, Y., Narzisi, G., Leotta, A., Grabowska, E. *et al.* (2012) De novo gene disruption in children on the autistic spectrum. *Neuron*, **74**, 285–299.
60. Samocha, K.E., Robinson, E.B., Sanders, S.J., Stevens, C., Sabo, A., McGrath, L.M., Kosmicki, J.A., Rehnström, K., Mallick, S., Kirby, A. *et al.* (2014) A framework for the interpretation of de novo mutation in human disease. *Nat. Genet.*, **46**, 944–950.

61. Lek, M., Karczewski, K.J., Minikel, E.V., Samocha, K.E., Banks, E., Fennell, T., O'Donnell-Luria, A.H., Ware, J.S., Hill, A.J., Cummings, B.B. *et al*. (2016) Analysis of protein-coding genetic variation in 60, 706 humans. *Nature*, **536**, 285–291.
62. Peng, Y.J., He, W.Q., Tang, J., Tao, T., Chen, C., Gao, Y.Q., Zhang, W.C., He, X.Y., Dai, Y.Y., Zhu, N.C. *et al*. (2010) Trio is a key guanine nucleotide exchange factor coordinating regulation of the migration and morphogenesis of granule cells in the developing cerebellum. *J. Biol. Chem.*, **285**, 24834–24844.
63. Zong, W., Liu, S., Wang, X., Zhang, J., Zhang, T., Liu, Z., Wang, D., Zhang, A., Zhu, M. and Gao, J. (2015) Trio gene is required for mouse learning and memorizing. *Brain Res.*, **1608**, 82–90.
64. Goebbels, S., Bormuth, I., Bode, U., Hermanson, O., Schwab, M.H. and Nave, K.A. (2006) Genetic targeting of principal neurons in neocortex and hippocampus of NEX-Cre mice. *Genesis*, **44**, 611–621.
65. Tilgner, H., Jahanbani, F., Blauwkamp, T., Moshrefi, A., Jaeger, E., Chen, F., Harel, I., Bustamante, C.D., Rasmussen, M. and Snyder, M.P. (2015) Comprehensive transcriptome analysis using synthetic long-read sequencing reveals molecular co-association of distant splicing events. *Nat. Biotechnol.*, **33**, 736–742.
66. van Zundert, B., Yoshii, A. and Constantine-Paton, M. (2004) Receptor compartmentalization and trafficking at glutamate synapses: a developmental proposal. *Trends Neurosci.*, **27**, 428–437.
67. Miller, M.B., Yan, Y., Wu, Y., Hao, B., Mains, R.E. and Eipper, B.A. (2016) Alternate promoter usage generates two subpopulations of the neuronal RhoGEF Kalirin-7. *J. Neurochem.*, 10.1111/jnc.13749.
68. Awasaki, T., Saito, M., Sone, M., Suzuki, E., Sakai, R., Ito, K. and Hama, C. (2000) The Drosophila trio plays an essential role in patterning of axons by regulating their directional extension. *Neuron*, **26**, 119–131.
69. Liebl, E.C., Forsthoefel, D.J., Franco, L.S., Sample, S.H., Hess, J.E., Cowger, J.A., Chandler, M.P., Shupert, A.M. and Seeger, M.A. (2000) Dosage-sensitive, reciprocal genetic interactions between the Abl tyrosine kinase and the putative GEF trio reveal trio's role in axon pathfinding. *Neuron*, **26**, 107–118.
70. Bateman, J., Shu, H. and Van Vactor, D. (2000) The guanine nucleotide exchange factor trio mediates axonal development in the Drosophila embryo. *Neuron*, **26**, 93–106.
71. Govek, E., Newey, S.E. and Van Aelst, L. (2005) The role of the Rho GTPases in neuronal development. *Genes Dev.*, **19**, 1–49.
72. Das, S., Yin, T., Yang, Q., Zhang, J., Wu, Y.I. and Yu, J. (2015) Single-molecule tracking of small GTPase Rac1 uncovers spatial regulation of membrane translocation and mechanism for polarized signaling. *Proc. Natl. Acad. Sci. U.S.A.*, **112**, E267–E276.
73. Yan, Y., Eipper, B.A. and Mains, R.E. (2016) Kalirin is required for BDNF-TrkB stimulated neurite outgrowth and branching. *Neuropharmacology*, **107**, 227–238.
74. Schiller, M.R., Ferraro, F., Wang, Y., Ma, X.-M., McPherson, C.E., Sobota, J.A., Schiller, N.I., Mains, R.E. and Eipper, B.A. (2008) Autonomous functions for the Sec14p/spectrin-repeat region of Kalirin. *Exp. Cell Res.*, **314**, 2674–2691.
75. Kannan, R., Song, J.-K., Karpova, T., Clarke, A., Shivalkar, M., Wang, B., Kotlyanskaya, L., Kuzina, I., Gu, Q. and Giniger, E. (2017) The Abl pathway bifurcates to balance Enabled and Rac signaling in axon patterning in *Drosophila*. *Development*, **144**, 487–498.
76. Lutz, S., Freichel-Blomquist, A., Yang, Y., Rümenapp, U., Jakobs, K.H., Schmidt, M. and Wieland, T. (2005) The guanine nucleotide exchange factor p63RhoGEF, a specific link between Gq/11-coupled receptor signaling and RhoA. *J. Biol. Chem.*, **280**, 11134–11139.
77. Rojas, R.J., Yohe, M.E., Gershburg, S., Kawano, T., Kozasa, T. and Sondek, J. (2007) Galphaq directly activates p63RhoGEF and Trio via a conserved extension of the Dbl homology-associated pleckstrin homology domain. *J. Biol. Chem.*, **282**, 29201–29210.
78. Lutz, S., Shankaranarayanan, A., Coco, C., Ridilla, M., Nance, M.R., Vettel, C., Baltus, D., Evelyn, C.R., Neubig, R.R., Wieland, T. *et al*. (2007) Structure of Galphaq-p63RhoGEF-RhoA complex reveals a pathway for the activation of RhoA by GPCRs. *Science*, **318**, 1923–1927.
79. van Unen, J., Reinhard, N.R., Yin, T., Wu, Y.I., Postma, M., Gadella, T.W.J. and Goedhart, J. (2015) Plasma membrane restricted RhoGEF activity is sufficient for RhoA-mediated actin polymerization. *Sci. Rep.*, **5**, 14693.
80. Borjigin, J. and Nathans, J. (1994) Insertional mutagenesis as a probe of rhodopsin's topography, stability, and activity. *J. Biol. Chem.*, **269**, 14715–14722.
81. Harlow, E. and Lane, D. (1988) *Antibodies: A Laboratory Manual*. Cold Spring Harbor Laboratory Press.
82. Yan, Y., Eipper, B.A. and Mains, R.E. (2015) Kalirin-9 and Kalirin-12 Play Essential Roles in Dendritic Outgrowth and Branching. *Cereb. Cortex*, **25**, 3487–3501.